On the ionized flux fraction and ion recycling in high power impulse magnetron sputtering

J. T. Guðmundsson[1,2], H. Hajihoseini[2,3], Alexandre Butler[3], Martin Čada[4], Zdeněk Hubička[4], Nils Brenning[1,3,5], Michael A Raadu[1], Tiberiu Minea[3], and Daniel Lundin[3,5]

[1] Department of Space and Plasma Physics, School of Electrical Engineering, KTH Royal Institute of Technology, Stockholm, Sweden
[2] Science Institute, University of Iceland, Reykjavik, Iceland
[3] Laboratoire de Physique des Gaz et Plasmas - LPGP, CNRS, Université Paris-Sud, Orsay, France
[4] Institute of Physics v. v. i., Academy of Sciences of the Czech Republic, Prague, Czech Republic
[5] Plasma and Coatings Physics, IFM-Materials Physics, Linköping University, Sweden

Satellite Workshop of XXXIV International Conference on Phenomena in Ionized Gases (XXXIV ICPIG) and the 10th International Conference on Reactive Plasmas (ICRP-10):
New trends of plasma processes for thin films and related materials
Sapporo, Japan, July 20., 2019

Introduction – Magnetron sputtering

- Magnetron sputtering has been a highly sucessfull technique that is essential in a number of industrial applications

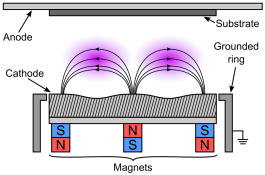

- Conventional dc magnetron sputtering (dcMS) suffers from a low degree of ionization of the sputtered material
- High power impulse magnetron sputtering (HiPIMS) provides a highly ionized material flux, while being compatible with conventional magnetron sputtering deposition systems

Introduction – HiPIMS

- High ionization of sputtered material requires very high density plasma
- In a conventional dc magnetron sputtering discharge the power density (plasma density) is limited by the thermal load on the target
- High power pulsed magnetron sputtering (HPPMS)
- In a HiPIMS discharge a high power pulse is supplied for a short period
  - low frequency
  - low duty cycle
  - low average power

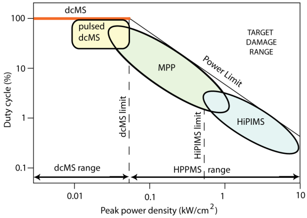

Gudmundsson et al. (2012) JVSTA **30** 030801

- Power density limits
  $p_t = 0.05$ kW/cm^2 dcMS limit
  $p_t = 0.5$ kW/cm^2 HiPIMS limit

Introduction – fraction of ionization

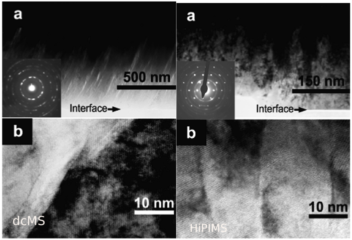

dc magnetron HiPIMS

After Alami et al. (2005) JVSTA, **23** 278

- In HiPIMS deposition, the high fraction of ionization of the sputtered species has been shown to lead to
  - the growth of smooth and dense films
  - enable control over their phase composition and microstructure
  - enhance mechanical and optical properties
  - improving film adhesion
  - enabling deposition of uniform films on complex-shaped substrates
- For optimization of HiPIMS thin film deposition processes, quantification and control of the fraction of ionization of the sputtered species are for obvious reasons key requirements

Introduction – fraction of ionization

- The effect of ionization fraction on the epitaxial growth of Cu film on Cu(111) substrate explored using Molecular Dynamics simulation
- Three deposition methods
  - thermal evaporation, fully neutral
  - dcMS, 50 % ionized
  - HiPIMS, 100 % ionized
- Higher ionization fraction of the deposition flux leads to smoother surfaces by two major mechanisms
  - decreasing clustering in the vapor phase
  - bicollision of high energy ions at the film surface that prevents island growth to become dominant

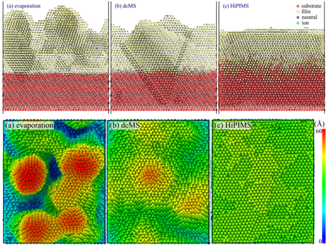

After Kateb et al. (2019) JVSTA, **37** 031306

Ionization region model studies of HiPIMS discharges

Ionization region model of HiPIMS

- The ionization region model (IRM) was developed to improve the understanding of the plasma behaviour during a HiPIMS pulse and the afterglow
- The main feature of the model is that an ionization region (IR) is defined next to the race track
- The IR is defined as an annular cylinder with outer radii r_{c2}, inner radii r_{c1} and length $L = z_2 - z_1$, extends from z_1 to z_2 axially away from the target

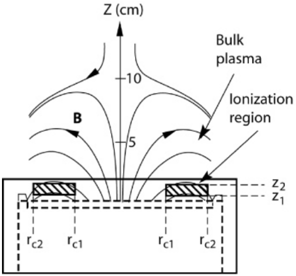

The definition of the volume covered by the IRM

From Raadu et al. (2011) PSST **20** 065007

Ionization region model of HiPIMS

- The temporal development is defined by a set of ordinary differential equations giving the first time derivatives of
  - the electron energy
  - the particle densities for all the particles
- The species assumed in the of-IRM are
  - cold electrons e^{C} (Maxwellian), hot electrons e^{H} (sheath acceleration)
  - argon atoms Ar($3s^2 3p^6$), warm argon atoms in the ground state Ar^{W}, hot argon atoms in the ground state Ar^{H}, Ar^{m} ($1s_5$ and $1s_3$) (11.6 eV), argon ions Ar^{+} (15.76 eV)
  - titanium atoms Ti(a ^{3}F), titanium ions Ti^{+} (6.83 eV), doubly ionized titanium ions Ti^{2+} (13.58 eV)
  - aluminium atoms Al($^2P_{1/2}$), aluminium ions Al^{+} (5.99 eV), doubly ionized aluminium ions Al^{2+} (18.8 eV)

Detailed model description is given in Huo et al. (2017) JPD **50** 354003

Ionization region model of HiPIMS

- The model is constrained by experimental data input and fitted to reproduce the measured discharge current and voltage curves, $I_{\rm D}(t)$ and $V_{\rm D}(t)$, respectively
- Two model fitting parameters were found to be sufficient for a discharge with Al target
  - $V_{\rm IR}$ accounts for the power transfer to the electrons
  - β is the probability of back-attraction of ions to the target

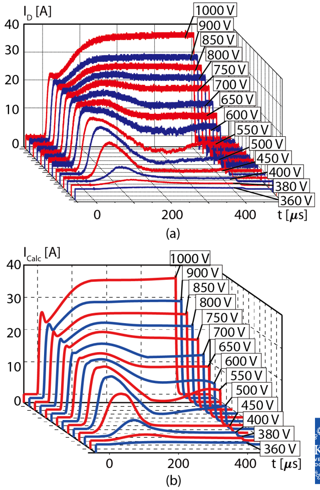

From Huo et al. (2017) JPD **50** 354003

Experimental data from Anders et al. (2007) JAP **102** 113303

Ionization region model of HiPIMS

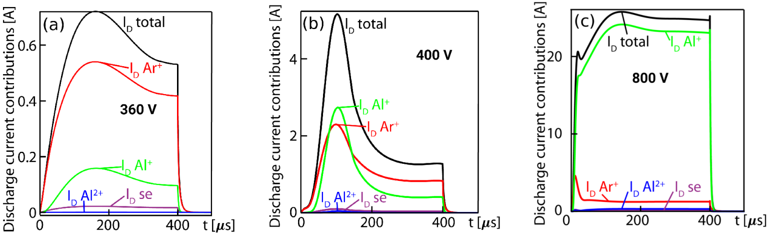

- A **non-reactive** discharge with 50 mm diameter Al target
- Current composition at the target surface

From Huo et al. (2017) JPD **50** 354003

Experimental data from Anders et al. (2007) JAP **102** 113303

Ionization region model of HiPIMS

- When the discharge is operated at 400 V the contributions of Al^{+} and Ar^{+}-ions to the discharge current are very similar
- At 800 V Al^{+}-ions dominate the discharge current (**self-sputtering**) while the contribution of Ar^{+} is below 10 % except at the initiation of the pulse

From Huo et al. (2017) JPD **50** 354003

Experimental data from Anders et al. (2007) JAP **102** 113303

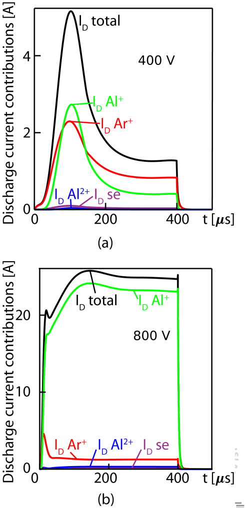

Ionization region model of HiPIMS

- A primary current I_{prim} is defined as ions of the working gas, here Ar^{+}, that are ionized for the first time and then drawn to the target
- This is the dominating current in dc magnetron sputtering discharges
- This current has a critical upper limit

$$I_{\mathrm{crit}} = S_{\mathrm{RT}} e p_{\mathrm{g}} \sqrt{\frac{1}{2\pi m_{\mathrm{g}} k_{\mathrm{B}} T_{\mathrm{g}}}} = S_{\mathrm{RT}} e n_{\mathrm{g}} \sqrt{\frac{k_{\mathrm{B}} T_{\mathrm{g}}}{2\pi m_{\mathrm{g}}}}$$

- Discharge currents I_{D} above I_{crit} are only possible if there is some kind of recycling of atoms that leave the target, become subsequently ionized and then are drawn back to the target

Anders et al. (2012) JPD **45** 012003

Huo et al. (2014) PSST **23** 025017

Ionization region model of HiPIMS

- For the 50 mm diameter Al target the critical current is $I_{\rm crit} \approx 7$ A
- The experiment is operated from far below $I_{\rm crit}$ to high above it, up to 36 A.
- With increasing current $I_{\rm prim}$ gradually becomes a very small fraction of the total discharge current $I_{\rm D}$
- The current becomes mainly carried by singly charged Al^{+}-ions, meaning that **self-sputter recycling** or the current $I_{\rm SS-recycle}$ dominates

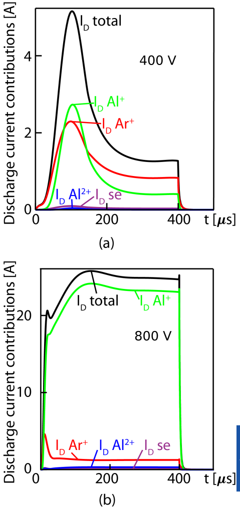

From Huo et al. (2017) JPD **50** 354003

Experimental data from Anders et al. (2007) JAP **102** 113303

Ionization region model of HiPIMS

- Recall that singly charged metal ions cannot create the secondary electrons – for metal self-sputtering (γ_{SE} is practically zero)
- The first ionization energies of many metals are insufficient to overcome the workfunction of the target material
- For the discharge with Al target operated at high voltage, self-sputter dominated, the effective secondary electron emission is essentially zero

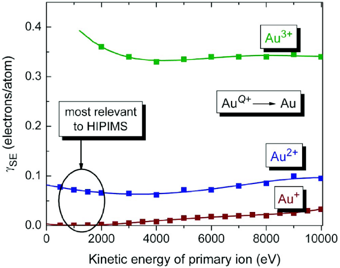

From Anders (2008) APL **92** 201501

Ionization region model of HiPIMS

- **Reactive** HiPIMS
- Ar/O_2 discharge with Ti target
- In the metal mode Ar^+ and Ti^+-ions contribute roughly equally to the current – combined **self-sputter recycling** and **working gas recycling**
- In the poisoned mode the current increaes and Ar^+-ions dominate the current – **working gas recycling**

From Gudmundsson et al. (2016) PSST **25**(6) 065004

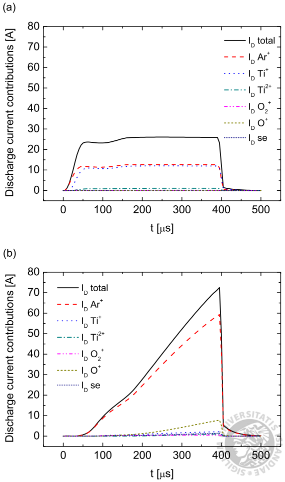

Ionization region model of HiPIMS

- Recycling map for five different targets with varying self-sputter yield
  - Cu – $Y_{SS} = 2.6$
  - Al – $Y_{SS} = 1.1$
  - Ti – $Y_{SS} = 0.7$
  - C – $Y_{SS} = 0.5$
  - TiO_2 – $Y_{SS} = 0.04 - 0.25$
- For very high self-sputter yields $Y_{SS} > 1$, the discharges above I_{crit} are of **type A** with dominating **SS-recycling**
- For very low self-sputter yields $Y_{SS} < 0.2$, the discharges above I_{crit} are of **type B** with dominating **working gas recycling**

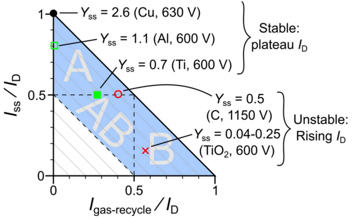

From Brenning et al. (2017),

PSST **26** 125003

Ionization region model of HiPIMS

- For the Al target, Ohmic heating is in the range of 87 % (360 V) to 99 % (1000 V)
- The domination of Al^{+}-ions, which have zero secondary electron emission yield, has the consequence that there is negligible sheath energization
- The ionization threshold for twice ionized Al^{2+}, 18.8 eV, is so high that few such ions are produced

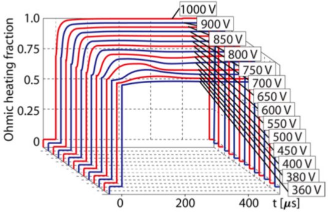

From Huo et al. (2017) JPD **50** 354003

Ionization region model of HiPIMS

- For a Ti target Ohmic heating is about 92 %
  - Both Ar^{+} and Ti^{2+}-ions contribute to creation of secondary electrons
- For Ti target in Ar/O_2 mixture
  - In the metal mode Ohmic heating is found to be 90 % during the plateau phase of the discharge pulse
  - For the poisoned mode Ohmic heating is 70 % with a decreasing trend, at the end of the pulse

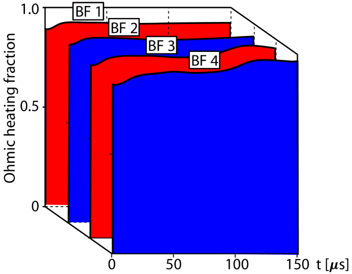

From Huo et al. (2017) JPD **50** 354003

Fraction of ionization

Fraction of ionization

- Quantification and control of the fraction of ionization of the sputtered species are crucial in magnetron sputtering
- We distinguish between three approaches to describe the degree (or fraction) of ionization
  - the ionized flux fraction

$$F_{\mathrm{flux}} = \frac{\Gamma_{\mathrm{i}}}{\Gamma_{\mathrm{i}} + \Gamma_{\mathrm{n}}}$$

  - the ionized density fraction

$$F_{\mathrm{density}} = \frac{n_{\mathrm{i}}}{n_{\mathrm{i}} + n_{\mathrm{n}}}$$

  - the fraction α of the sputtered metal atoms that become ionized in the plasma (probability of ionization)

Fraction of ionization

- There have been conflicting reports on the ionized flux fraction F_{flux}
  - 70 % for Cu (Kouznetsov et al., 1999)
  - 40 % for $Ti_{0.5}Al_{0.5}$ (Macak et al., 2000)
  - 9.5 % for Al (DeKoven et al., 2003)
  - 4.5 % for C (DeKoven et al., 2003)
  - 20 – 60 % for Ti (Kubart et al., 2014)
  - 20 – 68 % for Ti (Lundin et al., 2015)
- The degree of ionization F_{density}
  - 90 % for Ti (Bohlmark et al., 2005)
- The ionization flux fraction depends on applied power, discharge current density, pulse frequency and pulse length and the magnetic field strength

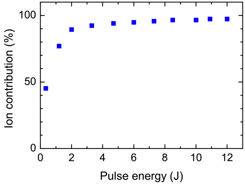

From Bohlmark et al. (2005) JVSTA **23** 18

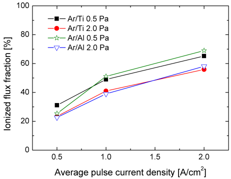

From Lundin et al. (2015) PSST **24** 035018

Fraction of ionization

- There have been a number of reports demonstrating the lower deposition rate in HiPIMS when compared to dcMS operated at the same average power (Helmersson et al., 2006; Anders, 2010).
- Samuelsson et al. (2010) compared the deposition rates from eight metal targets (Ti, Cr, Zr, Al, Cu, Ta, Pt, Ag) in pure Ar for both dcMS and HiPIMS discharges applying the same average power
- They observed that the HiPIMS deposition rates were in the range of 30 – 85% of the dcMS rates depending on target material.

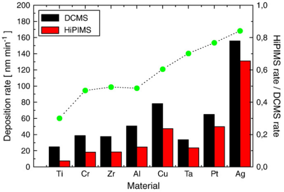

From Samuelsson et al. (2010) SCT **202** 591

Influence of magnetic field

Influence of magnetic field – Deposition rate

- The magnetic field distribution above the target for seven different magnet configurations: C0E0, C5E5 and C10E10, C0E5, C0E10, C5E0, and C10E
- For the configurations investigated, it was found that a magnetic null point was always present, which means that all configurations ware categorized as unbalanced type II
- The magnetic null was used as a measure of the degree of balancing and is in the range 43–74 mm from the target surface above the target center

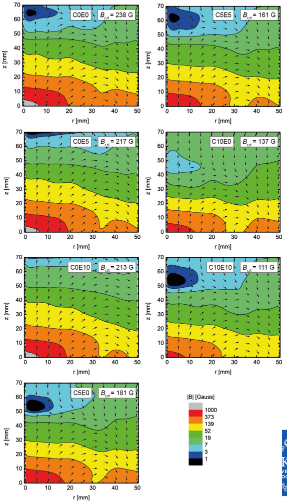

Influence of magnetic field – Deposition rate

- The HiPIMS discharge current and voltage waveforms recorded for various magnetic field configurations
  - (a) the discharge voltage in fixed voltage mode
  - (b) the discharge current in fixed voltage mode
  - (c) discharge current in fixed peak current mode
- The Ar pressure was set to 1 Pa
- In all cases the pulse width was 100 μs at an average power of 300 W

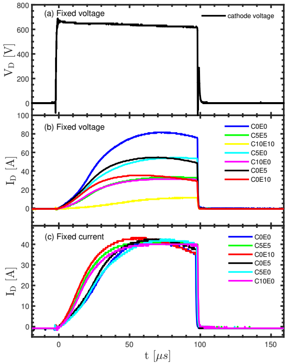

From Hajihoseini et al. (2019) *Plasma* **2** 201

Influence of magnetic field – Deposition rate

- The Ti deposition rate from both dcMS and HiPIMS discharges operated in fixed voltage mode and fixed current mode using various magnetic field configurations measured at 70 mm axial distance over center of cathode
- The magnet configurations on the $x-$axis are ordered from high $|\mathbf{B}|$ at the left to low $|\mathbf{B}|$ on the right
- The recorded $|B_{r,\mathrm{rt}}|$ value above the race track is used as a measure of $|\mathbf{B}|$

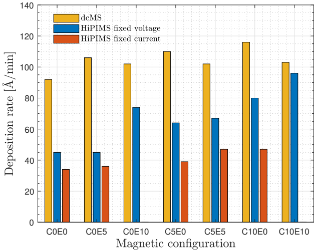

From Hajihoseini et al. (2019) *Plasma* **2** 201

Influence of magnetic field – Deposition rate

- The Ti ionized flux fraction in a HiPIMS discharge using various magnet configurations measured at 70 mm axial distance over the center of the cathode
- The magnet configurations on the $x-$axis are ordered from high $|\mathbf{B}|$ at the left to low $|\mathbf{B}|$ on the right
- The recorded $|B_{r,\mathrm{rt}}|$ value above the race track is used as a measure of $|\mathbf{B}|$

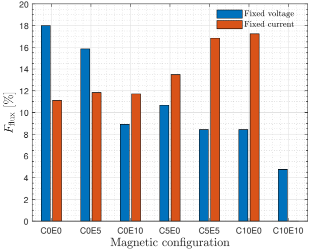

From Hajihoseini et al. (2019) *Plasma* **2** 201

Influence of magnetic field – Deposition rate

- The ionized flux fraction decreases with decreasing |**B**| when the HiPIMS discharge is operated in fixed voltage mode
- When operating in fixed peak current mode the ionized flux fraction F_{flux} increases slightly with decreasing |**B**|
- In this case ionized flux fraction increases from 11% to 16.8% when comparing cases C0E0 and C5E5 (no data from C10E10), i.e. by a factor 1.5 when decreasing |**B**|

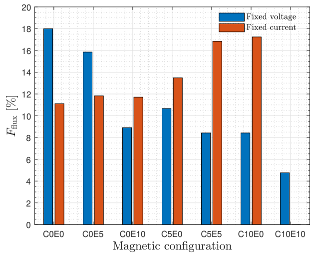

From Hajihoseini et al. (2019) *Plasma* **2** 201

Influence of magnetic field – Deposition rate

- We derive a few general equations that relate the measured quantities deposition rate and the ionized flux fraction to the parameters α_{t} and β_{t}
- Let us call the total flux (atoms/s) of atoms sputtered from the target Γ_0 and the flux of sputtered species (ions and neutrals) that leave the ionization region (IR) towards the diffusion region (DR) Γ_{DR}
- The useful fraction of the sputtered species becomes

$$F_{\mathrm{DR}} = \frac{\Gamma_{\mathrm{DR}}}{\Gamma_0} = (1 - \alpha_{\mathrm{t}}\beta_{\mathrm{t}})$$

- This equation indicates a reduced fraction of the sputtered species reaching the substrate when the ionization of the sputtered material increases

Influence of magnetic field – Deposition rate

- Recall that the main drawback using HiPIMS is the low deposition rate
- A relationship between the ionization flux fraction F_{flux} and the parameters α_{t} and β_{t} has been derived from the pathway model (Vlček and Burcalová, 2010; Butler et al., 2018)

$$F_{\mathrm{flux}} = \frac{\Gamma_{\mathrm{DR,ions}}}{\Gamma_{\mathrm{DR}}} = \frac{\Gamma_0 \alpha_{\mathrm{t}}(1-\beta_{\mathrm{t}})}{\Gamma_0(1-\alpha_{\mathrm{t}}\beta_{\mathrm{t}})} = \frac{\alpha_{\mathrm{t}}(1-\beta_{\mathrm{t}})}{(1-\alpha_{\mathrm{t}}\beta_{\mathrm{t}})}$$

  where no additional ionization of the sputtered material in the diffusion region is assumed
- Our goal is to assess how much $|\mathbf{B}|$ and the magnetic field structure influence α_{t} and β_{t}, repectively

Influence of magnetic field – Deposition rate

- A graph that shows F_{DR} on the horizontal axis, and F_{flux} on the vertical axis
- We have also plotted two sets of lines
  - lines of constant β_{t} with α_{t} varied from 0 to 1 (green dashed lines)
  - lines of constant α_{t}, with β_{t} varied from 0 to 1 (blue solid lines)
- Plotting the experimentally determined combinations of F_{DR} and F_{flux} in this plane gives us estimates of the corresponding values of α_{t} and β_{t}

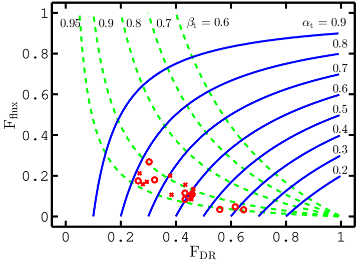

From Hajihoseini et al. (2019) *Plasma* **2** 201

Influence of magnetic field – Deposition rate

- We can derive an equation that gives the back attraction probability β_t as a function of the measured quantities F_{flux} and F_{DR}

$$\beta_t = \frac{1 - F_{DR}}{1 - F_{DR}(1 - F_{flux})}$$

and similarly we can derive an equation that gives α_t as a function of the measured quantities

$$\alpha_t = 1 - F_{DR}(1 - F_{flux}).$$

Influence of magnetic field – Deposition rate

- When operating in the fixed voltage mode (red) the ionization probability α_t increases with increased magnetic field strength
- When operating in the fixed peak current mode the ionization probability α_t is roughly constant independent of the magnetic field strength
- The back attraction probability is always high in the range 0.89 – 0.96 over the entire range of $B_{r,\mathrm{rt}}$

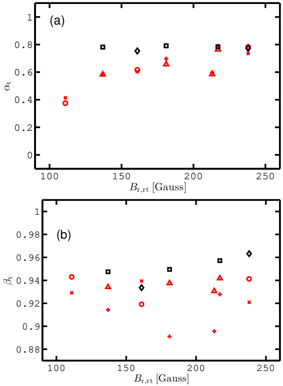

From Hajihoseini et al. (2019) *Plasma* 2 201

Influence of magnetic field – Deposition rate

- In the fixed peak current mode (**black**) $\beta_{\rm t}$ increases slightly with increased $|\mathbf{B}|$ in the range 0.93 – 0.96 while $\alpha_{\rm t}$ is almost constant in a narrow range 0.75 – 0.79
- If we assume a linear increase in $\beta_{\rm t}$ with $|\mathbf{B}|$ the fraction $(1-\beta_{\rm t})$ is roughly 30% higher at the highest $|\mathbf{B}|$ than at the lowest $|\mathbf{B}|$
- Recall that the total flux of ions of the sputtered material away from the target toward the substrate is $\Gamma_{\rm DR,ions} = \alpha_{\rm t}(1-\beta_{\rm t})\Gamma_0$

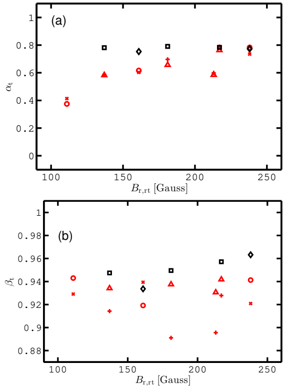

From Hajihoseini et al. (2019) *Plasma* **2** 201

Summary

Summary

- For high currents the discharge with Al target develops almost pure **self-sputter recycling**, while the discharge with Ti target exhibits close to a 50/50 combination of **self-sputter recycling** and **working gas-recycling**
- For very high self-sputter yields, above approximately $Y_{\rm SS} \approx 1$, the discharges above $I_{\rm crit}$ are of type A with
  - dominating SS-recycling
  - very little secondary electron emission
  - little sheath energization of electrons
- For very low self-sputter yields, below approximately $Y_{\rm SS} \approx 0.2$, the discharges above $I_{\rm crit}$ are of type B with
  - dominating working gas recycling
  - significant secondary electron emission
  - significant sheath energization of electrons.
- The fraction of the total electron heating that is attributable to Ohmic heating is over 90 % in the HiPIMS discharge

Summary

- For HiPIMS in the fixed voltage mode: A trade-off between the deposition rate (decreases by more than a factor of two) and the ionized flux fraction (increases by a factor 4 to 5) with increasing $|\mathbf{B}|$
- For HiPIMS in the fixed peak current mode: Decreasing $|\mathbf{B}|$ improves both the deposition rate (by 40%) and the ionized flux fraction (by 60%)
- When operating in the fixed peak current mode the ionization probability of the sputtered species is roughly constant while the parameter $(1 - \beta_\mathrm{t})$ increases roughly 30% with decreasing $|\mathbf{B}|$
- When operating a HiPIMS discharge in fixed voltage mode the ionization probability α_t is varied by $|\mathbf{B}|$ and β_t remains roughly constant, while in the fixed peak current mode β_t varies with $|\mathbf{B}|$ and α_t remains roughly constant

Thank you for your attention

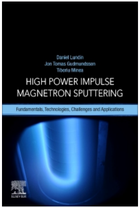

The slides can be downloaded at

`http://langmuir.raunvis.hi.is/~tumi/ranns.html`

and the project is funded by

- Icelandic Research Fund Grant Nos. 130029 and 196141

References

Alami, J., P. O. A. Petersson, D. Music, J. T. Gudmundsson, J. Bohlmark, and U. Helmersson (2005). Ion-assisted physical vapor deposition for enhanced film deposition on non-flat surfaces. *Journal of Vacuum Science and Technology A 23*(2), 278–280.

Anders, A., J. Andersson, and A. Ehiasarian (2007). High power impulse magnetron sputtering: Current-voltage-time characteristics indicate the onset of sustained self-sputtering. *J. Appl. Phys.* **102**(11), 113303.

Anders, A. (2008). Self-sputtering runaway in high power impulse magnetron sputtering: The role of secondary electrons and multiply charged metal ions. *Appl. Phys. Lett.* **92**(20), 201501.

Anders, A. (2010). Deposition rates of high power impulse magnetron sputtering: Physics and economics. *Journal of Vacuum Science and Technology A 28*(4), 783–790.

Anders, A., J. Čapek, M. Hála, and L. Martinu (2012). The 'recycling trap': a generalized explanation of discharge runaway in high-power impulse magnetron sputtering. *J. Phys D: Appl. Phys.* **45**(1), 012003.

Bohlmark, J., J. Alami, C. Christou, A. P. Ehiasarian, and U. Helmersson (2005). Ionization of sputtered metals in high power pulsed magnetron sputtering. *Journal of Vacuum Science and Technology A 23*(1), 18–22.

Brenning, N., J. T. Gudmundsson, M. A. Raadu, T. J. Petty, T. Minea, and D. Lundin, (2017). A unified treatment of self-sputtering, process gas recycling, and runaway for high power impulse sputtering magnetrons. *Plasma Sources Sci. Technol.* **26**(12), 125003.

Butler, A., N. Brenning, M. A. Raadu, J. T. Gudmundsson, T. Minea, and D. Lundin (2018). On three different ways to quantify the degree of ionization in sputtering magnetrons. *Plasma Sources Science and Technology 27*(10), 105005.

DeKoven, B. M., P. R. Ward, R. E. Weiss, D. J. Christie, R. A. Scholl, W. D. Sproul, F. Tomasel, and A. Anders (2003). Carbon thin film deposition using high power pulsed magnetron sputtering. In *Society of Vacuum Coaters 46th Annual Technical Conference Proceedings*, San Francisco, CA, USA, pp. 158–165. Society of Vacuum Coaters.

Gudmundsson, J. T., N. Brenning, D. Lundin, and U. Helmersson (2012). The high power impulse magnetron sputtering discharge. *Journal of Vacuum Science and Technology A 30*(3), 030801.

Gudmundsson, J. T., D. Lundin, N. Brenning, M. A. Raadu, C. Huo, and T. M. Minea (2016). An ionization region model of the reactive Ar/O_2 high power impulse magnetron sputtering discharge. *Plasma Sources Science and Technology* **25**(6), 065004.

References

Hajihoseini, H., M. Čada, Z. Hubička, S. Ünaldi, M. A. Raadu, N. Brenning, J. T. Gudmundsson, and D. Lundin (2019). The effect of magnetic field strength and geometry on the deposition rate and ionized flux fraction in the HiPIMS discharge. *Plasma 2*(2), 201–221.

Helmersson, U., M. Lattemann, J. Bohlmark, A. P. Ehiasarian, and J. T. Gudmundsson (2006). Ionized physical vapor deposition (IPVD): A review of technology and applications. *Thin Solid Films 513*(1-2), 1–24.

Huo, C., D. Lundin, J. T. Gudmundsson, M. A. Raadu, J. W. Bradley, and N. Brenning (2017). Particle-balance models for pulsed sputtering magnetrons. *J. Phys. D: Appl. Phys.* **50**(35), 354003.

Huo, C., D. Lundin, M. A. Raadu, A. Anders, J. T. Gudmundsson, and N. Brenning (2014). On the road to self-sputtering in high power impulse magnetron sputtering: particle balance and discharge characteristics. *Plasma Sources Sci. Technol.* **23**(2), 025017.

Kateb, M., H. Hajihoseini, J. T. Gudmundsson, and S. Ingvarsson (2019). Role of ionization fraction on the surface roughness, density, and interface mixing of the films deposited by thermal evaporation, dc magnetron sputtering, and HiPIMS: An atomistic simulation. *Journal of Vacuum Science and Technology A 37*(3), 031306.

Kouznetsov, V., K. Macák, J. M. Schneider, U. Helmersson, and I. Petrov (1999). A novel pulsed magnetron sputter technique utilizing very high target power densities. *Surface and Coatings Technology 122*(2-3), 290–293.

Kubart, T., M. Čada, D. Lundin, and Z. Hubička (2014). Investigation of ionized metal flux fraction in HiPIMS discharges with Ti and Ni targets. *Surface and Coatings Technology 238*, 152–157.

Lundin, D., M. Čada, and Z. Hubička (2015). Ionization of sputtered Ti, Al, and C coupled with plasma characterization in HiPIMS. *Plasma Sources Science and Technology 24*(3), 035018.

Macak, K., V. Kouznetsov, J. Schneider, U. Helmersson, and I. Petrov (2000). Ionized sputter deposition using an extremely high plasma density pulsed magnetron discharge. *Journal of Vacuum Science and Technology A 18*(4), 1533 – 1537.

Raadu, M. A., I. Axnäs, J. T. Gudmundsson, C. Huo, and N. Brenning (2011). An ionization region model for high power impulse magnetron sputtering discharges. *Plasma Sources Sci. Technol.* **20**(6), 065007.

Samuelsson, M., D. Lundin, J. Jensen, M. A. Raadu, J. T. Gudmundsson, and U. Helmersson (2010). On the film density using high power impulse magnetron sputtering. *Surface and Coatings Technology 202*(2), 591–596.

Vlček, J. and K. Burcalová (2010). A phenomenological equilibrium model applicable to high-power pulsed magnetron sputtering. *Plasma Sources Science and Technology 19*(6), 065010.